A New Universal Isolated Converter for Grid Connection

Myoungho Kim, *Student Member, IEEE*, Anno Yoo, *Member, IEEE*, and Seung-Ki Sul, *Fellow, IEEE*

***Abstract*—This paper proposes an isolated universal-link ac–ac power converter suitable for grid connection. The proposed power converter can have multiple ports to connect various loads or electric energy sources, and the configuration can be arranged according to the situation. The proposed power converter does not need to employ the large interface inductor at input side and the huge electrolytic capacitor at dc link. Moreover, it utilizes high-frequency transformers for the galvanic isolation instead of bulky line-frequency transformers. These characteristics of the proposed power converter result in the reduction of the system volume and weight remarkably. The proposed power converter is the modular structure, and an H-bridge works as a basic module of the converter. By stacking the modules, the power converter can be adapted to the high-voltage grid and the various types of loads and/or sources. This paper addresses the structure of the proposed power converter and the fundamental principle of power flow. The operation of the proposed converter is verified by both computer simulations and experimental results with a laboratory-level prototype system.**

***Index Terms*—AC–AC power converter, bidirectional power flow, grid connection, HF transformers, renewable energy source.**

I. Introduction

RENEWABLE energy has been appreciated as alternative resources for electric power generation. As fossil fuel prices soar and environmental issues are concerned, the installations of renewable energy have continued growing dramatically around the world. Also, the advances in technologies have led the power capacity of the renewable energy system to grow [1]–[4]. However, it can be a problem to integrate the renewable energy sources to the conventional grid in terms of the grid stability, voltage regulation, and power quality issues. Renewable energies inherently have uncertainty in their nature. For example, the output power, voltage, and frequency of the wind turbine depend on the speed of wind, which fluctuate over time and cannot be forecasted accurately. Therefore, the renewable energy sources cannot be connected to the grid directly. In order to interface the renewable energy sources to the grid, a suitable power converter is required. The requirements for the grid-connected power converter can be listed as follows:

1) galvanic isolation between the grid and the energy sources for protection and safety;
2) preferring bidirectional power flow capability;
3) control of reactive power transfer between the grid and the energy sources;
4) high quality of the injected power into the grid;
5) variable-frequency operation including dc for the renewable energy sources.

Many studies have been done about the converter topologies which fulfill the aforementioned requirements for interfacing the renewable energy sources to the grid.

The neutral point clamped (NPC) converter [5] and the flying capacitor converter [8] are well known in this field. These topologies are able to synthesize higher number of output voltage levels, which makes it possible to reduce the voltage and current harmonics applied to the grid. However, the number of the output voltage level is limited for practical applications because of the many issues, such as complexity of the structure and difficulty of the regulation of the dc-link capacitor voltages. Modified or hybrid versions of these topologies, namely, the three-level active NPC [9] and five-level active NPC [10] topologies, has been developed to reduce these difficulties. These topologies are mainly employed as three to five level converters.

The other classical topology is the cascaded H-bridge (CHB) converter [11], [12], which is constituted by the series-connected H-bridge converters. It is suitable for high-voltage high-power application because of its modular structure. However, it requires complex phase-shifted input transformer to supply isolated dc sources. This makes the CHB converter expensive and bulky, so the CHB topology is seldom employed in the lower power applications. The modular multilevel converter (MMC) [13], [14] also has modularity. It consists of series-connected half-bridge power cells. Like the CHB topology, the MMC can be easily adopted to the high-voltage system due to its modularity and scalability.

All the aforementioned converter topologies employ the heavy line-frequency transformer for galvanic isolation and the bulky capacitors at the dc link. These large reactive components increase the system volume and maintenance cost. In particular, the electrolytic capacitors at dc link deteriorate the reliability of the system owing to its shorter life expectancy.

Manuscript received May 5, 2011; revised July 8, 2011 and September 25, 2011; accepted November 2, 2011. Date of publication December 20, 2011; date of current version March 21, 2012. Paper 2011-IPCC-153.R2, presented at the 2010 IEEE Energy Conversion Congress and Exposition, Atlanta, GA, September 12–16, and approved for publication in the IEEE Transactions on Industry Applications by the Industrial Power Converter Committee of the IEEE Industry Applications Society.

M. Kim and S.-K. Sul are with the School of Electrical Engineering and Computer Science, Seoul National University, Seoul 151-744, Korea (e-mail: myoungho@eepel.snu.ac.kr; sulsk@plaza.snu.ac.kr).

A. Yoo is with LSIS Co., Ltd., Anyang-si 431-080, Korea (e-mail: ayoo@lsis.biz).

Color versions of one or more of the figures in this paper are available online at http://ieeexplore.ieee.org.

Digital Object Identifier 10.1109/TIA.2011.2180496

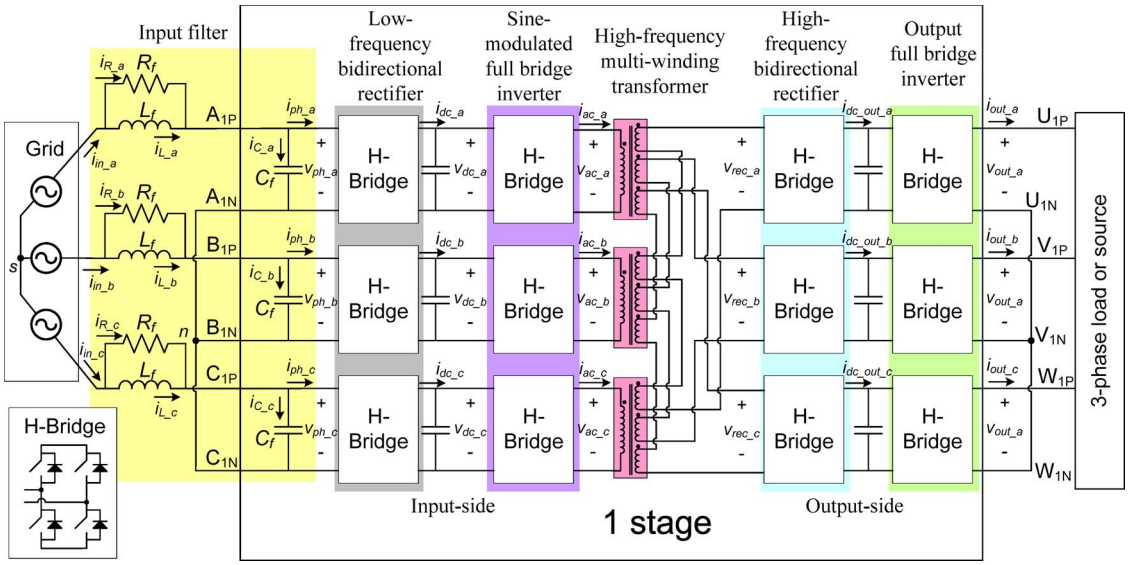

Fig. 1. Basic configuration of the proposed series-connected universal-link converter.

To overcome the issues related to the reactive components and to connect the power converter to the grid directly, the multilevel matrix converter has been investigated [15]. It does not require passive energy storage, such as inductor or capacitors. Accordingly, the volume and the weight of the converter can be reduced. However, the voltage utilization ratio of the matrix converter is reduced on the average sense compared to the other voltage source inverter. Moreover, the large line-frequency transformer is required for the galvanic isolation.

Some other studies have been performed to utilize a high-frequency transformer for isolation instead of the line-frequency transformer [16]–[21]. A dual active bridge (DAB) converter was introduced at first in [16], and this topology has been used widely in high-power dc–dc converters owing to its advantages of high-power density, isolation characteristic, bidirectional power transfer capability, and modular and simple structure [17], [18]. The concept of the DAB has extended to the various applications from the simple dc–dc converters. In [19], the DAB circuit is suggested as a building block of a flexible power converter which can be connected to various energy sources and/or loads. The high-frequency transformer can reduce the volume of the system considerably. Using this concept, Watson *et al.* [21] proposed the universal flexible power management system. It is capable of interfacing different grids and various sources/loads. However, this topology still requires large dc-link capacitors at the grid side for input current shaping.

This paper proposes SEries-connected Output Universal Link converter (SEOUL converter) for the connection of grid to various energy sources and/or loads. The converter is capable of bidirectional power flow and displacement power factor (DPF) control. The size of the converter can be reduced because it does not require any bulky reactive components such as the electrolytic capacitors and the huge line-frequency transformers. The grid current waveform is sinusoidal without high-frequency operation of the input-side converter. As a result of the modular nature of the structure, the modules can be connected in different configurations to accommodate various sources and loads for increased voltage and power levels.

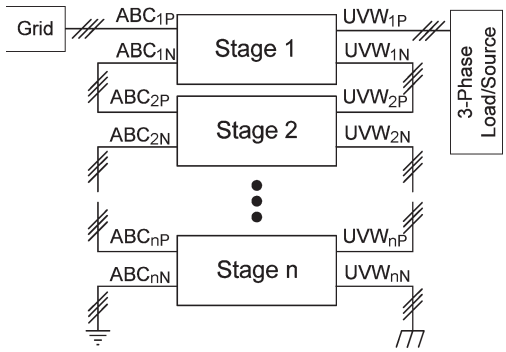

Fig. 2. Series connection structure of SEOUL converter.

This paper is organized as follows. Section II introduces a basic structure of the proposed converter. The operating principle is described in Section III. Some simulation results are presented in Section IV. Section V presents experimental results with a laboratory prototype to validate the operation of the proposed converter. Section VI shows the possibility of the extension of the proposed SEOUL converter. Finally, the conclusions are noted in Section VII.

II. Structure of the SEOUL Converter

Fig. 1 shows the basic structure of the SEOUL converter. It has one grid-connected input port and one three-phase output port. Each input/output port consists of H-bridge module, and the modules are connected in Y-connection to the grid and the source/load, respectively. The circuit in Fig. 1 is named as a stage. Each module of the same phase in a stage can be connected in series to accommodate higher input or output voltage as shown in Fig. 2. The number of stage is determined depending on the dc-link voltage level of one H-bridge module and input ac voltage level.

The H-bridges configuring the proposed converter are classified into four types according to their operations, namely,

low-frequency bidirectional rectifier, sine-modulated full-bridge inverter, high-frequency bidirectional rectifier, and output full-bridge inverter.

The low-frequency bidirectional rectifier is configured similar to the electrolytic capacitor-less inverter [22], [23]. It acts as a bidirectional ac–dc interface without any energy storage components at the dc link except small snubber capacitors to decouple the stray inductances of the dc link and semiconductor itself. Using only small capacitors at the dc link, the input currents can be kept as sinusoidal one naturally in contrast to current shaping through high-frequency switching of conventional pulsewidth modulation (PWM) boost converter.

The filter capacitors in the grid side help distribute the phase voltage evenly across the stages, if the multiple stages are connected in series. The capacitors also function as input filter along with filter inductance to suppress the high-frequency current ripples coming from the sine-modulated full-bridge inverter. The switches of the low-frequency bidirectional rectifier are switched synchronously with the line frequency; hence, their switching frequency is the same to the line frequency, and the switching loss of the low-frequency bidirectional rectifier is negligible.

The sine-modulated full-bridge inverter and the high-frequency bidirectional rectifier are connected to the high-frequency multiwinding transformer. They perform isolated bidirectional power conversion analogous to the DAB converter [16]. The galvanic isolation between the input and output ports is achieved with the high-frequency transformers. The switching frequency of H-bridges in this part can be set up to 10 kHz considering the capacity of the existing switching devices. Therefore, the size of the transformer used in this converter is much smaller than that of conventional line-frequency transformers used in other topologies.

The transformer has one winding on the primary side and multiwindings on the secondary side. The number of windings on the secondary side is determined by the number of phases of the output side. The secondary windings of the transformer are connected in series, which makes the voltage applied to the high-frequency bidirectional rectifier the sum of the primary-side voltages. With this circuit structure and the appropriate voltage synthesis, the power transferred through one transformer can be constant under the assumption of the balanced load. The dc outputs of the high-frequency bidirectional rectifier provide isolated dc voltage sources. Using them, the output full-bridge inverter is operated as a single cell of a CHB converter. Each H-bridge controls its output voltage independently.

The SEOUL converter can be adopted for high-voltage application. The converter can be stacked over stages due to the modular nature of the structure as shown in Fig. 2. The converter can link various systems to the high-voltage grid in this way.

III. Operating Principle

The SEOUL converter has a sinusoidal form of the input current without using the PWM boost converter. In this section, it is described how the input current is kept as sinusoidal without high-frequency switching.

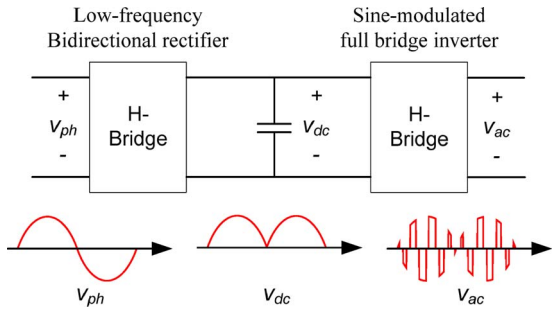

Fig. 3. Voltage waveforms of the input side.

A. Input-Side Voltage Modulation

In Fig. 3, the voltage waveforms of the input side of converter are shown conceptually. The input phase voltage has sinusoidal form, which is rectified by the low-frequency bidirectional rectifier. Hence, the dc-link voltage shapes as the absolute value of the sinusoidal waveform. Then, the sine-modulated full-bridge inverter chopped the dc-link voltage according to the output voltage reference. The details are described as follows.

First, the input phase voltage can be defined as follows:

$$\begin{aligned} v_{\mathrm{ph\_}a} &= V\ \sin(\omega\, t) \\ v_{\mathrm{ph\_}b} &= V\ \sin\left(\omega t - \frac{2}{3}\pi\right) \\ v_{\mathrm{ph\_}c} &= V\ \sin\left(\omega t + \frac{2}{3}\pi\right) \end{aligned} \tag{1}$$

where V is the magnitude of the phase voltage and ω is the angular frequency of the grid.

Each switch of the low-frequency bidirectional rectifier turns on when its antiparallel diode turns on. Then, the dc-link voltages of the input side become absolute value of input phase voltage because there are virtually no reactive components in the dc link. These voltages can be derived as follows:

$$\begin{aligned} v_{\mathrm{dc\_}a} &= V\,|\sin(\omega\, t)| \\ v_{\mathrm{dc\_}b} &= V\left|\sin\left(\omega t - \frac{2}{3}\pi\right)\right| \\ v_{\mathrm{dc\_}c} &= V\left|\sin\left(\omega t + \frac{2}{3}\pi\right)\right|. \end{aligned} \tag{2}$$

With the variable dc-link voltages, the sine-modulated full-bridge inverters synthesize their output voltages as follows:

$$\begin{aligned} v_{\mathrm{ac\_}a} &= mV\,|\sin(\omega t)|\ \mathrm{sign}\,(\sin(\omega t)) \\ &\quad \times \sin(\omega t - \varphi)\mathrm{square}(t) \\ v_{\mathrm{ac\_}b} &= mV\left|\sin\left(\omega t - \frac{2}{3}\pi\right)\right|\ \mathrm{sign}\left(\sin\left(\omega t - \frac{2}{3}\pi\right)\right) \\ &\quad \times \sin\left(\omega t - \frac{2}{3}\pi - \varphi\right)\mathrm{square}(t) \\ v_{\mathrm{ac\_}c} &= mV\left|\sin\left(\omega t + \frac{2}{3}\pi\right)\right|\ \mathrm{sign}\left(\sin\left(\omega t + \frac{2}{3}\pi\right)\right) \\ &\quad \times \sin\left(\omega t + \frac{2}{3}\pi - \varphi\right)\mathrm{square}(t) \end{aligned} \tag{3}$$

where m is the modulation index $(0 \le m \le 1)$, $\mathrm{square}(t)$ is the modulation function alternating between -1 and 1 with the switching frequency of the PWM, $\mathrm{sign}(x)$ is 1 when x is

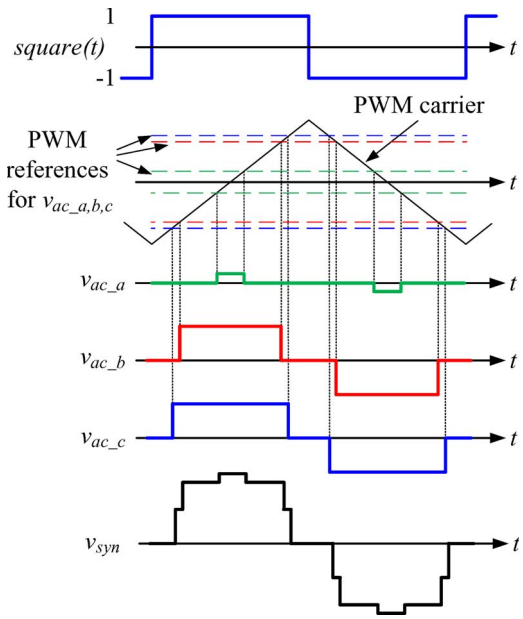

Fig. 4. Output voltage formation of the sine-modulated full-bridge inverters.

positive and -1 when x is negative, and φ is the desired DPF angle defined as the angle between the input phase voltage and current.

The voltage synthesis of the sine-modulated full-bridge inverter enables the input grid current of the SEOUL converter to be sinusoidal without any high-frequency switching of the low-frequency bidirectional rectifier. The output voltages of sine-modulated full-bridge inverter are applied to the primary side of the transformers, and the voltages applied to the high-frequency bidirectional rectifier are the sum of output voltages of the sine-modulated full-bridge inverters since the windings on secondary side of the transformer are connected in series. Assuming that the output voltages of the sine-modulated full-bridge inverters are balanced, the voltages applied to the high-frequency bidirectional rectifiers can be derived as follows:

$$\begin{aligned} v_{\text{syn}} &= n(v_{\text{ac\_}a} + v_{\text{ac\_}b} + v_{\text{ac\_}c}) \\ &= \frac{3}{2}mnV\ \cos(\varphi)\text{square}(t) \end{aligned} \tag{4}$$

where n is the turn ratio of the transformer. The turn ratio of primary and secondary sides can be set arbitrarily as $1:n$. As shown in (4), the effective voltage transferring to the secondary side is constant on the average sense because the nonconstant and time-varying components except "square(t)" are cancelled out due to the balanced input phase voltage.

Fig. 4 shows the synthesized output voltages of (3) and (4) at a certain switching period. The magnitudes of the output voltages are determined by each dc-link voltage, and the output duty ratios are set by PWM to match the reference (3). The summed voltage v_{syn} forms a staircase wave and varies according to the dc-link voltages at each switching instant. However, its average value is constant over the switching period.

B. High-Frequency Power Transfer

When the output-side dc-link voltage of the high-frequency bidirectional rectifier is constant, the power transferring through the high-frequency multiwinding transformer can be achieved in similar manner of the DAB converter [16]. It can be explained with an equivalent circuit, shown in Fig. 5. The equivalent circuit includes three-phase sine-modulated full-bridge inverters and three high-frequency transformers with one output winding and one high-frequency bidirectional rectifier. This equivalent circuit can be modeled from the point of view of the output side of the transformer. In the circuit, "v_{syn}" is the sum of the output voltages of the sine-modulated full-bridge inverter, considering transformer turn ratio, and "v_{rec}" is the output voltage of the high-frequency bidirectional rectifier. It has a form of bipolar square wave phase shifted from the function "square(t)" of the sine-modulated full-bridge inverter by angle ϕ. "X" means the sum of leakage inductances of the three transformers. The approximate power transferring via the transformer in the switching frequency can be given as follows:

$$P = \frac{V_{s1}V_{r1}}{2X}\sin\phi \tag{5}$$

where V_{s1} and V_{r1} are the magnitudes of the fundamental frequency components, which are the switching frequencies of the sine-modulated full-bridge inverter, of the v_{syn} and v_{rec}, respectively. The angle ϕ is the phase-shift angle between the two voltage sources. In the proposed scheme, V_{s1} and V_{r1} are set by the voltage level of dc links and the modulation index of the v_{syn}, and the transferring power is controlled by adjusting the phase shift angle ϕ. Then, the output-side dc-link voltage can be controlled by transferring power control. Since the high-frequency power transfer part of the SEOUL converter is analogous to the DAB converter, it is expected that a soft switching would be achieved. However, due to the different winding connection and the voltage modulation, the soft-switching condition is relatively complex than that of the DAB converter. A detailed analysis of soft-switching condition would be a future work. An analysis for the multiport dc–dc converter [14] would be a good reference.

C. Output Side Control

The output full-bridge inverters share the dc link with the high-frequency bidirectional rectifiers, and they synthesize each single-phase ac output voltage. Assuming that the ac load is balanced, the output phase voltage synthesized by the inverters and current to each output full-bridge inverter can be defined as follows:

$$\begin{aligned} v_{\text{out\_}a} &= V_o\sin(\omega_o t) \\ v_{\text{out\_}b} &= V_o\sin\left(\omega_o t - \frac{2}{3}\pi\right) \\ v_{\text{out\_}c} &= V_o\sin\left(\omega_o t + \frac{2}{3}\pi\right) \end{aligned} \tag{6}$$

$$\begin{aligned} i_{\text{out\_}a} &= I_o\sin(\omega_o t - \psi) \\ i_{\text{out\_}b} &= I_o\sin\left(\omega_o t - \frac{2}{3}\pi - \psi\right) \\ i_{\text{out\_}c} &= I_o\sin\left(\omega_o t + \frac{2}{3}\pi - \psi\right) \end{aligned} \tag{7}$$

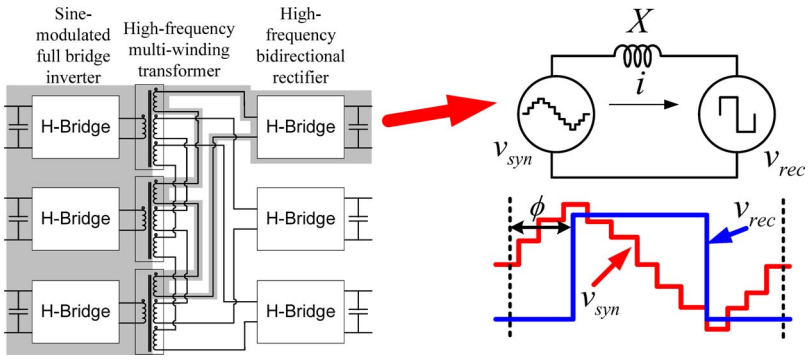

Fig. 5. Equivalent circuit of the high-frequency power transfer part.

where V_o and I_o are the magnitudes of the output voltage and current, and ψ is the phase difference between output voltage and current. Then, considering the power balance, the output-side dc-link currents can be derived as follows:

$$\begin{aligned} i_{\mathrm{dc\_out\_}a} &= \frac{V_o I_o}{2V_{\mathrm{dco}}}\left[\cos(\psi) - \cos(2\omega_o t + \psi)\right] \\ i_{\mathrm{dc\_out\_}b} &= \frac{V_o I_o}{2V_{\mathrm{dco}}}\left[\cos(\psi) - \cos\left(2\omega_o t - \frac{2}{3}\pi + \psi\right)\right] \\ i_{\mathrm{dc\_out\_}c} &= \frac{V_o I_o}{2V_{\mathrm{dco}}}\left[\cos(\psi) - \cos\left(2\omega_o t + \frac{2}{3}\pi + \psi\right)\right] \end{aligned} \quad (8)$$

where V_{dco} is the output-side dc-link voltages. These currents flow into the secondary side of the transformer. They have fluctuating component with twice of output frequency because of single-phase ac output. However, these fluctuating currents are not transferred to the primary side of the high-frequency transformer as they are cancelled as a result of the connection of the secondary windings to each phase. Therefore, the current flowing into the sine-modulated full-bridge inverters can be simplified to a form of pure square wave as follows:

$$i_{\mathrm{ac\_}a,b,c} \approx I_{\mathrm{dc}}\mathrm{square}(t) \quad (9)$$

where I_{dc} is constant, and it is deduced as $V_o I_o \cos(\psi)/mV\cos(\varphi)$, considering the power balance between primary and secondary sides.

Considering the modulation of the sine-modulated full-bridge inverters by (3) and the instantaneous power balance, the dc-link current flowing into the low-frequency bidirectional rectifiers can be derived as follows:

$$\begin{aligned} i_{\mathrm{dc\_}a} &= mI_{\mathrm{dc}}\sin(\omega t - \varphi)\mathrm{sign}\left(\sin(\omega t)\right) \\ i_{\mathrm{dc\_}b} &= mI_{\mathrm{dc}}\sin\left(\omega t - \frac{2}{3}\pi - \varphi\right)\mathrm{sign}\left(\sin\left(\omega t - \frac{2}{3}\pi\right)\right) \\ i_{\mathrm{dc\_}c} &= mI_{\mathrm{dc}}\sin\left(\omega t + \frac{2}{3}\pi - \varphi\right)\mathrm{sign}\left(\sin\left(\omega t + \frac{2}{3}\pi\right)\right). \end{aligned} \quad (10)$$

Then, by the operation of the low-frequency bidirectional rectifier, the waveform of the input phase current of the converter would be the sinusoidal one with desired DPF angle φ as shown in

$$\begin{aligned} i_{\mathrm{ph\_}a} &= I\sin(\omega t - \varphi) \\ i_{\mathrm{ph\_}b} &= I\sin\left(\omega t - \frac{2}{3}\pi - \varphi\right) \\ i_{\mathrm{ph\_}c} &= I\sin\left(\omega t + \frac{2}{3}\pi - \varphi\right), \quad \text{where } I = mI_{\mathrm{dc}}. \end{aligned} \quad (11)$$

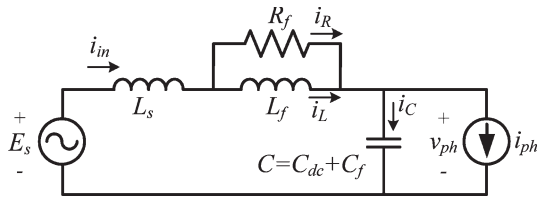

Fig. 6. Simplified single-phase equivalent circuit of the proposed converter from the point of view of the grid.

Equation (11) only presents the fundamental frequency component of the input phase current of the low-frequency bidirectional rectifier. However, there also exist high-frequency components in the input phase current. The high-frequency switching operation of the proposed converter causes the switching current, and most of it is transferred to the phase input grid current because the proposed converter has only small snubber capacitors on its dc links. Therefore, a filter is required to prevent the high-frequency current from being transferred to the grid.

D. Input Filter Design

The proposed converter employs an input filter which consists of $L-C$ and a damping resistor. Fig. 6 shows the simplified single-phase equivalent circuit. In Fig. 6, E_s and L_s represent the phase voltage and the line inductance of the grid. R_f, L_f, and C_f are a damping resistor, an input filter inductor, and a filter capacitor, respectively. C_{dc} is the input-side dc-link capacitance. The complete SEOUL converter, connected after the input filter, can be modeled as a current source i_{ph} for the design of the input filter. The cutoff frequency of the filter is given in

$$\omega_c = \frac{1}{\sqrt{L_F C}}. \quad (12)$$

In order to suppress the switching current transferring into the grid, the cutoff frequency of the filter should be set as a fraction of the switching frequency of the converter. L_f should be more than several times of L_s to set the cutoff frequency accurately regardless of the line inductance. The damping resistor is determined to have the same impedance of L_f to maximize the damping effect at the cutoff frequency of the filter, as shown in (13) [23]

$$R_f = \omega_c L_f. \quad (13)$$

The filter capacitors also help distribute the phase voltage evenly across the stages. When the converter is connected in series, as shown in Fig. 2, the voltages applied to the filter capacitors across the stages in the same phase may be different. Larger filter capacitor helps in balancing the voltage across each stage. Harmonics or unbalance in the load may lead the phase voltage to be unbalanced. Then, the balanced power flow would be deteriorated because the voltage synthesis of the sine-modulated full-bridge inverter is under the assumption that the phase voltage of the converter is balanced. Larger filter capacitor is beneficial for the phase voltage balancing. However, increasing the filter capacitor leads the filter inductor to be reduced with a fixed cutoff frequency. The filter parameters L_f and C_f should be chosen properly considering these issues.

E. Control Strategy

A phase-locked loop (PLL) is used to acquire the phase angle of the input phase voltage. The voltage modulation of input side is based on this phase angle. The switching operation of the low-frequency bidirectional rectifiers is synchronized to the phase angle. Also, the output pulsewidth of the sine-modulated full-bridge inverters is decided with the phase angle.

The input power factor of the proposed converter is determined by the desired DPF angle φ in (3). However, the grid phase current $i_{\rm in}$ is different from the input phase current of the converter $i_{\rm ph}$ because of the input filter. The current flowing into the capacitor of the input filter in Fig. 6 i_C affects the grid phase current. Assuming that the voltage across the filter inductance is small enough to neglect, the grid phase current can be derived as follows:

$$\begin{aligned} i_{\rm in} &= i_C + i_{\rm ph} = C\frac{d}{dt}v_{\rm ph} + i_{\rm ph} \\ &= \sqrt{(\omega CV - I\sin\varphi)^2 + (I\cos\varphi)^2}\,\sin(\omega t - \delta) \end{aligned} \quad (14)$$

where

$$\delta = \tan^{-1}\left(\frac{I\sin\varphi - \omega CV}{I\cos\varphi}\right)$$

$$E_s \approx v_{\rm ph} = V\sin(\omega t) \quad i_{\rm ph} = I\sin(\omega t - \varphi).$$

The phase angle between "$i_{\rm in}$" and "$i_{\rm ph}$" can be different according to the size of the filter capacitor and the load current. The DPF angle at the grid δ can be controlled by adjusting the desired DPF angle at the sine-modulated full-bridge inverter as derived in (3).

The output-side dc-link voltage is regulated as constant with a voltage controller. The dc-link voltage is controlled by controlling the power flowing through the high-frequency transformer. The power transferring via the transformer is determined by V_{s1}, V_{r1}, and ϕ, as shown in (5). Among the three variables, the voltage controller adjusts the phase-shift angle ϕ only. Another variable V_{s1} is set by the input-side dc-link voltage level, which depends on the input phase voltage and the modulation index m which is set as 0.8 in this paper to reduce the transferring power fluctuation [24]. The other variable V_{r1} is dependent on the output-side dc-link voltage, which is constant.

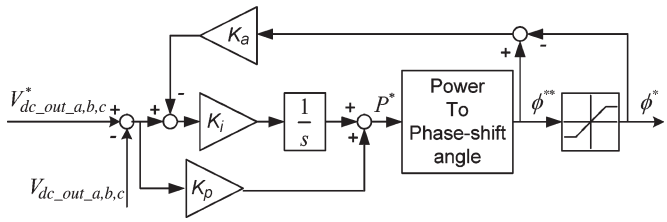

Fig. 7. Block diagram of the output-side dc-link voltage controller.

TABLE I
PARAMETERS OF THE SIMULATION

Quantity	Value [Unit]
Grid voltage	3300 [V], 60 [Hz]
Load/source voltage	3300 [V], 60 [Hz]
Input filter parameters	L_F; 1 [mH] C_F; 450 [μF] R_F; 2.6 [Ω]
Input-side DC-link capacitor	30 [μF]
Output-side DC-link capacitor	10,000 [μF]
Switching frequency of sine-modulated full bridge inverter and output full bridge inverter	2 [kHz]

Fig. 7 shows the structure of the output-side dc-link voltage controller. A proportional and integral (PI) controller is employed for each phase separately. A PI controller adjusts the transferring power command, in accordance with the error between the reference voltage and the measured voltage. The power reference is converted to the phase-shift angle using (5).

Another PLL is employed to acquire the output-side phase angle, and using the output phase angle, a synchronous frame PI current generates the voltage references of the output full-bridge inverters. The output full-bridge inverters synthesize their output voltage to control the output current with the phase-shifted carrier PWM like the conventional CHB converter [12].

IV. Simulation Results

Simulations are performed to verify the feasibility of the proposed scheme in the case of the input ac voltage, which is 3300 $V_{\rm rms}$. The converter is supposed to link an independent three-phase voltage source to the grid. Both powering (the power flows from the grid to the output side) and regenerating (the power flows from the output side to the grid side) mode simulations are performed. The converter is rated at 3300 V, 60 Hz, and 1 MVA with series-connected three stages. The phase voltage applied to each stage is 898 V, and each H-bridge is composed of four 1700-V insulated-gate bipolar transistors (IGBTs). System parameters are given in Table I.

Fig. 8 shows the output voltage of a sine-modulated full-bridge inverter applied to the primary side of the transformer, which is described as (3). According to (3), the pulsewidth is

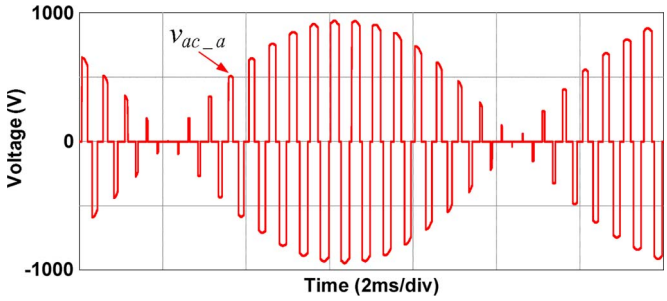

Fig. 8. Waveform of the output voltage of the sine-modulated full-bridge inverter (simulation).

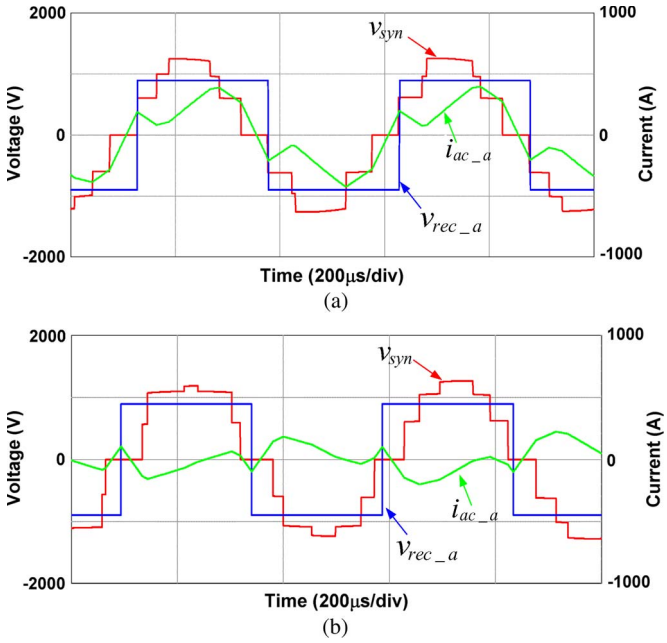

Fig. 9. Waveforms of the voltage and the current applied on the transformers (simulation). (a) Powering operation. (b) Regenerating operation.

supposed to be proportional to the magnitude of the dc-link voltage, and that can be verified in Fig. 8.

Fig. 9 shows the voltages applied to the high-frequency multiwinding transformer and current flowing through it. Both powering and regenerating operation results are displayed. This figure supports the power transfer concept shown in Fig. 5. The phase-shift angle between the voltages applied on primary and secondary sides of the transformer, namely, "$v_{\rm syn}$" and "$v_{\rm rec}$," determines the power flowing from sine-modulated full-bridge inverters to high-frequency bidirectional rectifiers through the transformer. The output-side dc-link voltage is regulated as 898 V, the same level of the input-side dc-link voltage.

Figs. 10 and 11 show the waveforms of the input phase voltage and current of the grid and those of the output phase voltage and current at powering and regenerating operations. In both cases, the amount of power is 700 kW each. The input phase current is sinusoidal, and the current at the output side is also well regulated. The input phase currents are lagging or leading to the phase voltage according to the power flow direction because of the effect of the input filter, as described in Section III-E. This can be compensated by the desired DPF angle control. Fig. 12 shows the results of the input DPF compensation. The DPF of the grid is controlled to unity by adjusting φ of the sine-modulated full-bridge inverters.

The simulation results demonstrate a feasibility of SEOUL converter for interfacing different frequency ac systems with bidirectional power flow capability at medium-voltage power transfer.

In Fig. 13, the estimated system efficiency is presented, calculated through the computer simulation. In this paper, the system loss is categorized into two parts, the semiconductor loss and the transformer loss. Any other losses such as capacitor loss and losses on the stray resistances are neglected. The semiconductor loss is calculated with "thermal module" of PSIM, a circuit simulation tool. It calculates the conduction and switching loss of the device considering the applied voltage and current on the device. The loss information required in the calculation is referred from the IGBT datasheet (FF300R17KE4 of Infineon). The transformer loss consists of core loss and the copper loss. The core loss is calculated by Stienmetz equation [25], and the copper loss is calculated using the simulation result of the rms current flowing through the transformer. Parameters of the transformer model used for the loss calculation are given in Table II.

The efficiency increases as the power increases. One of the main reasons of this is the soft-switching characteristic of the high-frequency power transfer part. As mentioned in Section III-B, the operation of the high-frequency power transfer is similar to the DAB converter [16]. The soft-switching characteristic of the SEOUL converter is analogous to that of the DAB converter too. As the power increases, which means that the phase-shift angle between the primary and the secondary side voltages increases, the more number of switches are able to be operated under zero voltage switching condition. The overall efficiency would increase as the power increases since the switching losses of the high-frequency parts take large portion of the total loss of SEOUL converter.

V. Experimental Results

This section presents the experimental setup and results to verify the operation of the proposed converter. The photograph of a prototype SEOUL converter is shown in Fig. 14. It consists of the input filter, 12 H-bridge modules, and three high-frequency multiwinding transformers to interface the three-phase grid input and three-phase output. The parameters of the prototype are given in Table III. The high-frequency multiwinding transformer is shown in Fig. 15. It uses a nanocrystalline toroidal core (FT-3KM of Hitachi) for high-power density. It has one primary winding and three secondary windings. The turn ratio is set as 3:2. The configuration of the experiment is shown in Fig. 16. The input port of the converter is linked to line-to-line 220-$V_{\rm rms}$ 60-Hz grid, and the output port is connected to the grid via a line-frequency transformer. The power is circulated through the converter and the line-frequency transformer.

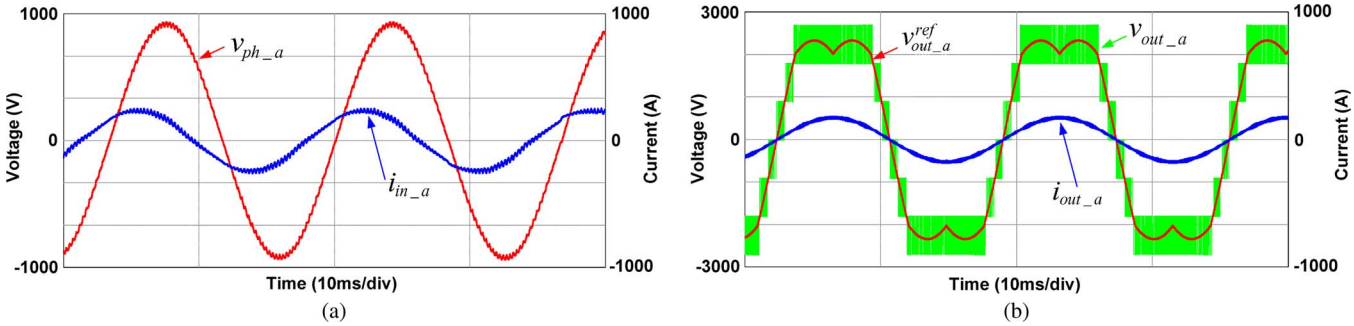

Fig. 10. Waveforms of the input and output phase voltages and currents at the powering operation (simulation). (a) Input phase voltage and current. (b) Output phase voltage and current.

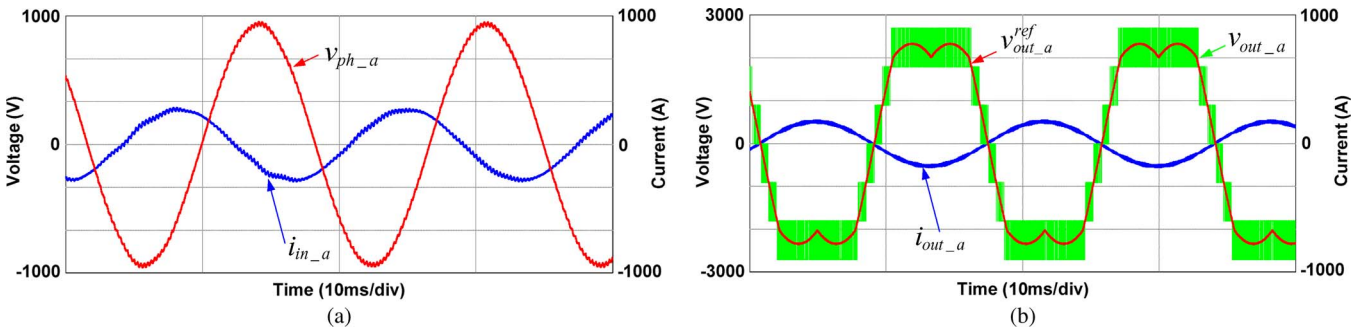

Fig. 11. Waveforms of the input and output phase voltages and currents at the regenerating operation (simulation). (a) Input phase voltage and current. (b) Output phase voltage and current.

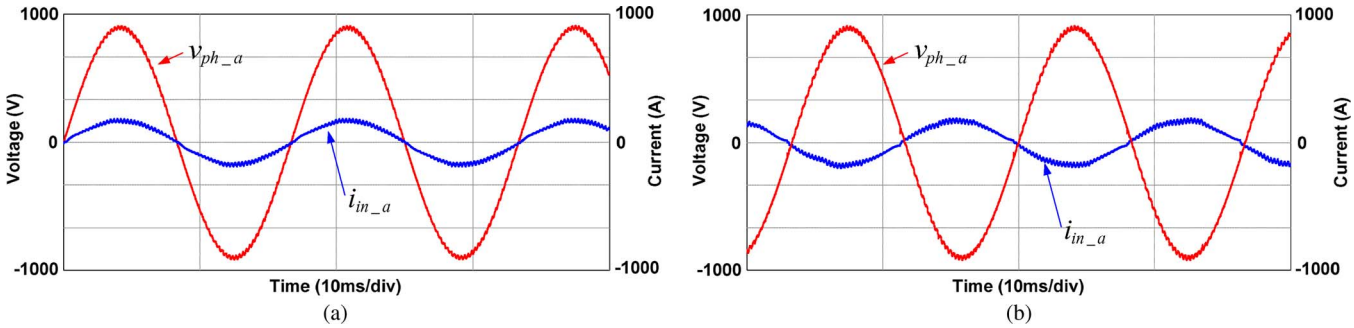

Fig. 12. Waveforms of the input phase voltages and currents with the input DPF control (simulation). (a) Powering operation. (b) Regenerating operation.

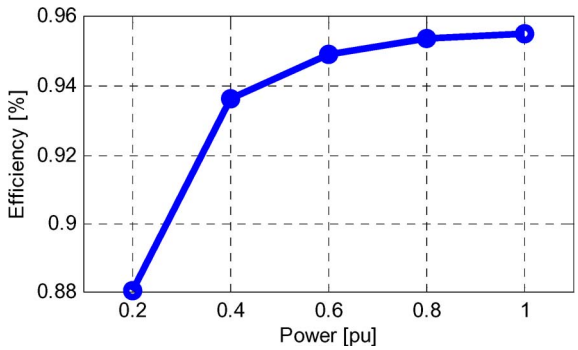

Fig. 13. Estimated overall system efficiency.

The secondary-side dc-link voltage is regulated as 180 V, same with the peak value of the primary-side dc-link voltage. In order to evaluate the bidirectional power capability, both powering and regenerating operations are performed.

TABLE II
PARAMETERS OF THE HIGH-FREQUENCY MULTIWINDING TRANSFORMER IN THE SIMULATION

Quantity	Value [Unit]
Rated Power	222 [kVA]
Rated Voltage	Primary ; 898 [V] Secondary ; 599 [V]
Rated Current	Primary ; 247 [A] Secondary ; 124 [A]
Turn Ratio	3 : 2
Winding Resistance (using Litz wire, calculated in switching frequency)	Primary ; 3.96 [mΩ] Secondary ; 3.08 [mΩ]
Core Material	Fe-based amorphous

The waveforms of the primary-side dc-link voltage and the output of the sine-modulated full-bridge inverter are shown in Fig. 17. The dc-link voltage is the absolute value of sine

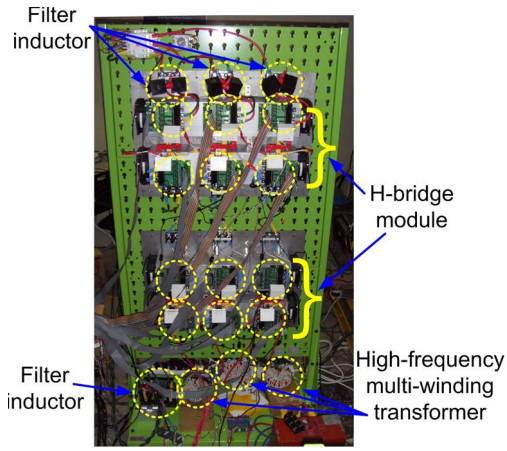

Fig. 14. Photograph of a prototype SEOUL converter.

TABLE III
PARAMETERS OF THE EXPERIMENT

Quantity	Value [Unit]
Grid voltage	220 [V], 60 [Hz]
Load/source voltage	220 [V], 60 [Hz]
Input filter parameters	L_F ; 100 [μH] C_F ; 100 [μF] R_F ; 1 [Ω]
Input-side DC-link capacitor	11 [μF]
Output-side DC-link capacitor	500 [μF]
Switching frequency of sine-modulated full bridge inverter and output full bridge inverter	10 [kHz]

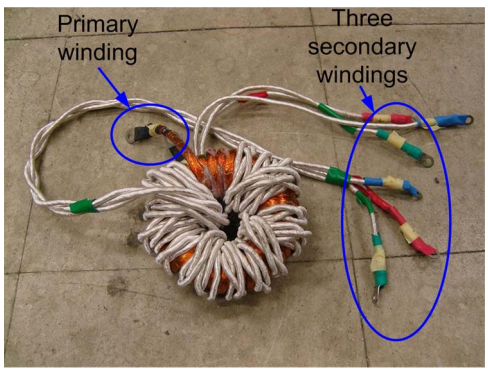

Fig. 15. Photograph of the high-frequency multiwinding transformer.

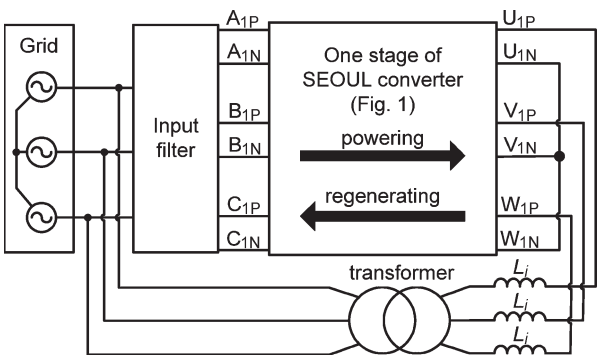

Fig. 16. Experimental configuration.

wave since the low-frequency bidirectional rectifier switches its conduction states according to the sign of the input phase voltage. Using dc-link voltage, the sine-modulated full-bridge inverter synthesizes its output voltage to meet the reference, as presented in (3). The magnified view in time scale clarifies that the pulsewidth varies proportionally to the magnitude of dc-link voltage.

The voltage and current waveforms applied on the high-frequency transformer at the powering and the regenerating operations are shown in Fig. 18(a) and (b), respectively. The primary transformer voltage imposed by each phase is a quasi-square wave. However, multilevel voltages actually observed as the quasi-square wave produced by each primary side cell are summed on the secondary side of the transformer. Therefore, the fundamental component of the effective voltage applied to the secondary side of the transformer is constant on the average sense for a switching period. As shown in (5), the power transfer via the transformer is performed by controlling the phase-shift angle ϕ. It can be seen that the phase-shift angle is changed in accordance with the direction of the power transfer.

The waveforms of the input and output phase voltages and currents on the powering and the regenerating operations are shown in Fig. 19(a) and (b), respectively. The amount of flowing power is 5.4 kW in both operations. The output current is controlled to be unity power factor by the output full-bridge inverters.

In Fig. 20, the desired DPF angle φ is set as null; hence, there are phase differences between the input phase voltage and the current due to the effect of the input filter. Fig. 18 shows the results of the DPF compensation. The desired DPF angle is adjusted to make the DPF of the grid be unity.

VI. EXPANDABILITY OF THE CONVERTER

One of the attractive features of the SEOUL converter is the expandability. Owing to its modular structure, the output port can be extended by changing the winding arrangement of the transformers and adding the H-bridges. For example, in order to link two separate three-phase systems to the grid, each transformer would have six secondary windings. Each winding is connected to the one phase of high-frequency bidirectional rectifier. They compose two separate three-phase output sides, which can be connected to a three-phase load or energy source individually. The dc-link voltages at the H-bridges of each output side can be set separately by modifying the turn ratio. In addition, dc loads or sources can be attached in similar manner. Fig. 21 shows an example of this expandability. One three-phase load and a dc load are attached to the output side. The transformer has four isolated secondary windings, and every single phase of H-bridge is connected to the separated secondary winding of the transformer.

VII. CONCLUSION

This paper has proposed the SEOUL converter as a power converter topology. The SEOUL converter may have multi-outputs supporting several bidirectional power flow sources

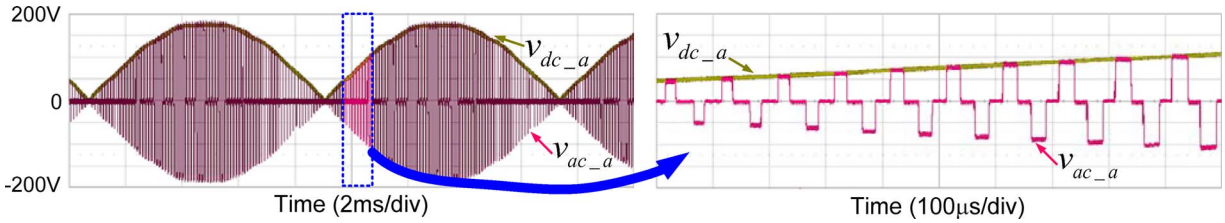

Fig. 17. Experimental waveforms of the output voltage of the sine-modulated full-bridge inverter.

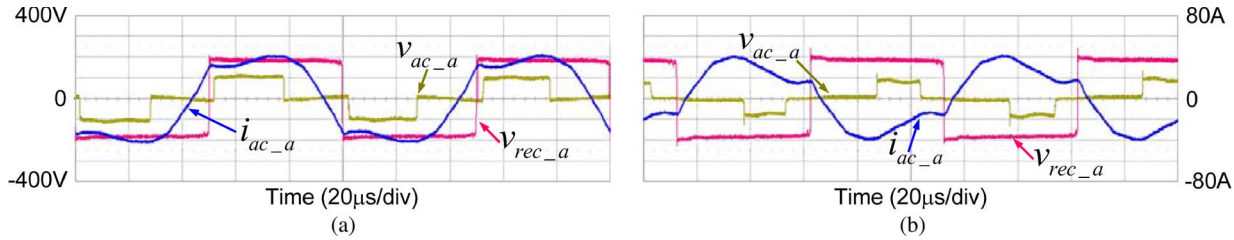

Fig. 18. Experimental waveforms of the voltage and the current applied on the transformers. (a) Powering operation. (b) Regenerating operation.

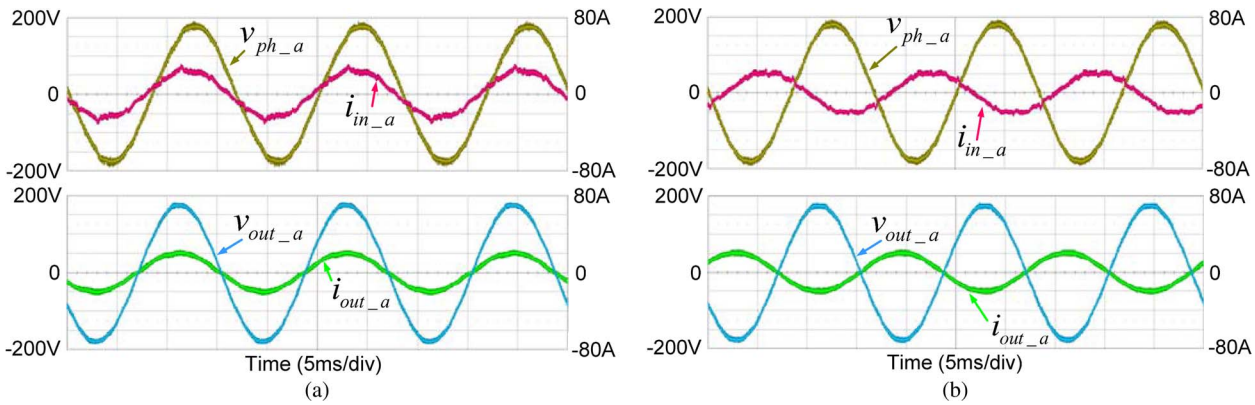

Fig. 19. Experimental waveforms of the input and output phase voltages and currents. (a) Powering operation. (b) Regenerating operation.

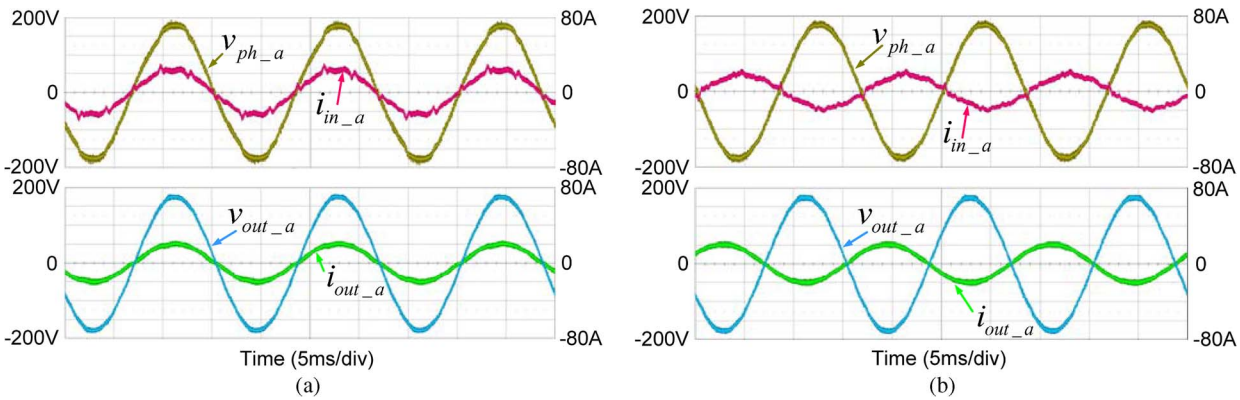

Fig. 20. Experimental waveforms of the input and output phase voltages and currents with the DPF control. (a) Powering operation. (b) Regenerating operation.

and loads. Both ac and dc loads and/or energy sources, such as a wind generator and fuel cells, can be linked simultaneously. The proposed converter is suitable for grid connection incorporating many renewable sources and energy storage system because of its flexibility. Also, the DPF at the grid side can be controlled. The converter utilizes the high-frequency transformer as the galvanic isolation instead of the heavy line-frequency transformer, which contributes to the reduction of the volume and the weight of the converter. The converter consists of H-bridge modules, and it is expected that the proposed power converter can be connected to medium voltage by stacking the H-bridge module in series. Additionally, by simple rearranging of transformers and H-bridges, output ports can be extended. With this feature, the SEOUL converter can be used as a building block for universal link of the renewable energy sources to the conventional grid. Some

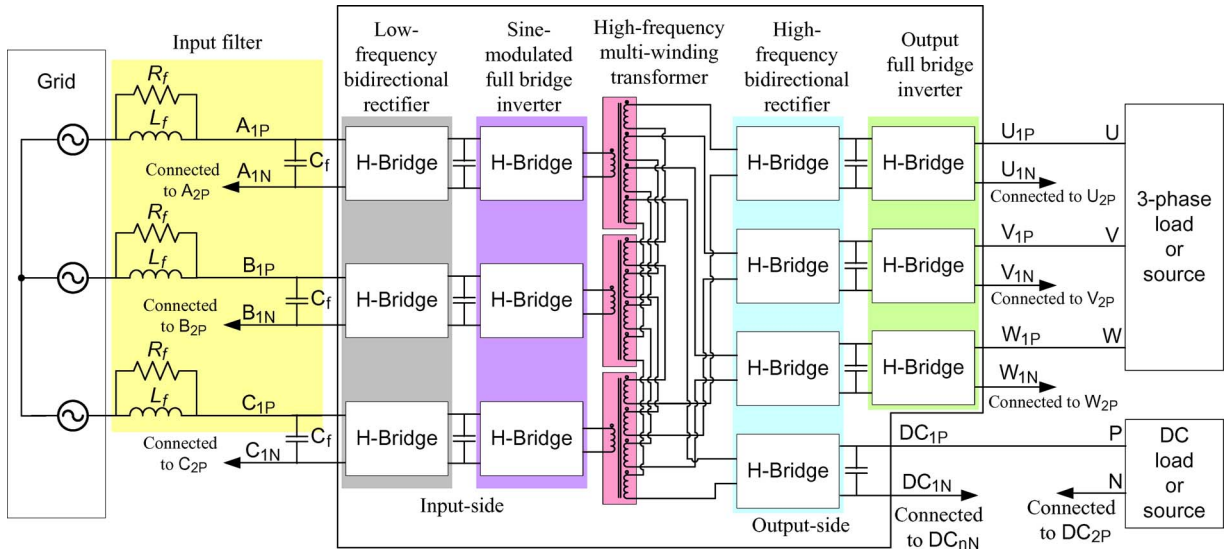

Fig. 21. Example of extended structure of SEOUL converter for a three-phase load and one dc load.

simulation and experimental results prove the validity of the control concept and the feasibility of the proposed SEOUL converter.

REFERENCES

[1] H. Bevrani, A. Ghosh, and G. Ledwich, "Renewable energy sources and frequency regulation: Survey and new perspectives," *IET Renew. Power Gener.*, vol. 4, no. 5, pp. 438–457, Sep. 2000.

[2] J. M. Carrasco, L. G. Franquelo, J. T. Bialasiewcz, E. Galvan, R. C. P. Guisado, M. A. M. Prats, J. I. Leon, and N. Moreno-Alfonso, "Power-electronic systems for the grid integration of renewable energy sources: A survey," *IEEE Trans. Ind. Appl.*, vol. 53, no. 4, pp. 1002–1016, Jul./Aug. 2006.

[3] F. Blaabjerg, R. Teodorescu, M. Liserre, and A. V. Timbus, "Overview of control and grid synchronization for distributed power generation systems," *IEEE Trans. Ind. Electron.*, vol. 53, no. 5, pp. 1398–1409, Oct. 2006.

[4] J. A. Baroudi, V. Dinavahi, and A. M. Knight, "A review of power converter topologies for wind generators," *Renew. Energy*, vol. 32, no. 14, pp. 2369–2385, Nov. 2007.

[5] A. Nabae, I. Takahashi, and H. Akagi, "A new neutral-point clamped PWM inverter," *IEEE Trans. Ind. Appl.*, vol. IA-17, no. 5, pp. 518–523, Sep. 1981.

[6] S. Aplepuz, S. Busquets-Monge, J. Bordonau, J. Gago, D. Gonzalez, and J. Balcells, "Interfacing renewable energy sources to the utility grid using a three-level inverter," *IEEE Trans. Ind. Electron.*, vol. 53, no. 5, pp. 1504–1511, Oct. 2006.

[7] A. Yazdani and R. Iravani, "A neutral-point clamped converter system for direct-drive variable-speed wind power unit," *IEEE Trans. Energy Convers.*, vol. 21, no. 2, pp. 596–607, Jun. 2006.

[8] T. A. Meynard and H. Foch, "Multi-level choppers for high voltage applications," in *Proc. Eur. Conf. Power Electron. Appl.*, 1992, pp. 45–50.

[9] O. Apeldoorn, B. Odegard, P. Steimer, and S. Bernet, "A 16 MVA ANPC-PEBB with 6 ka IGCTs," *Conf. Rec. 40th IEEE IAS Annu. Meeting*, vol. 2, no. Oct. 2–6, 2005, pp. 818–824.

[10] F. Kieferndorf, M. Basler, L. A. Serpa, J.-H. Fabian, A. Coccia, and G. A. Scheuer, "A new medium voltage drive system based on anpc-5l technology," in *Proc. IEEE-ICIT*, viña del Mar, Chile, Mar. 2010, pp. 605–611.

[11] P. W. Hammond, "A new approach to enhance power quality for medium voltage AC drives," *IEEE Trans. Ind. Appl.*, vol. 33, no. 1, pp. 202–208, Jan/Feb. 1997.

[12] M. A. Perez, J. R. Espinoza, J. R. Rodriguez, and P. Lezana, "Regenerative medium-voltage AC drive based on a multicell arrangement with reduced energy storage requirements," *IEEE Trans. Ind. Electron.*, vol. 52, no. 1, pp. 171–180, Feb. 2005.

[13] A. Lesnicar and R. Marquardt, "An innovative modular multilevel converter topology suitable for a wide power range," in *Proc. IEEE Powertech Conf.*, Bologna, Italy, 2003, pp. 1–6.

[14] B. Gemmell, J. Dorn, D. Retzmann, and D. Soerangr, "Prospects of multilevel VSC technologies for power transmission," in *Conf. Rec. IEEE-TDCE*, 2008, pp. 1–16.

[15] P. Wheeler, X. Lie, M. Y. Lee, L. Empringham, C. Klumpner, and J. Clare, "A review of multi-level matrix converter topologies," in *Proc. 4th IET Conf. PEMD*, Apr. 2–4, 2008, pp. 286–290.

[16] R. W. De Doncker, D. M. Divan, and M. H. Kheraluwala, "A three-phase soft-switched high power density DC/DC converter for high power applications," *IEEE Trans. Ind. Appl.*, vol. 27, no. 1, pp. 63–73, Jan/Feb. 1991.

[17] G. G. Oggier, L. P. Botalla, and G. O. García, "Soft-switching analysis for three-port bidirectional DC–DC converters," in *Proc. INDUSCON Conf.*, Sao Paulo, Brazil, 2010, pp. 1–6.

[18] E. Koutroulis, J. Chatzakis, K. Kalaitzaks, and N. C. Voulgaris, "A bidirectional, sinusoidal, high frequency inverter design," *Proc. Inst. Elect. Eng.—Elect. Power Appl.*, vol. 148, no. 4, pp. 315–321, Jul. 2001.

[19] S. Inoue and H. Akagi, "A bidirectional DC–DC converter for an energy storage system with galvanic isolation," *IEEE Trans. Power Electron.*, vol. 22, no. 6, pp. 2296–2306, Nov. 2007.

[20] S. Inoue and H. Akagi, "A bidirectional isolated DC–DC converter as a core circuit of the next-generation medium-voltage power conversion system," *IEEE Trans. Power Electron.*, vol. 22, no. 2, pp. 535–542, Mar. 2007.

[21] A. J. Watson, H. Q. S. Dang, G. Mondal, J. C. Clare, and P. W. Wheeler, "Experimental implementation of a multilevel converter for power system integration," in *Proc. IEEE-ECCE*, Sep. 2009, pp. 2232–2238.

[22] S. Kim, S. K. Sul, and T. A. Lipo, "AC/AC power conversion based on matrix converter topology with unidirectional switches," *IEEE Trans. Ind. Appl.*, vol. 36, no. 1, pp. 139–145, Jan./Feb. 2000.

[23] B. Piepenbreier and L. Sack, "Regenerative drive converter with line-frequency switched rectifier and without DC link component," in *Proc. 35th IEEE PESC*, Aachen, Germany, Jun. 20–25, 2004, pp. 3917–3923.

[24] A. Yoo, K. Kim, and S.-K. Sul, "Analysis of high-frequency power conversion for series-connected universal link AC/DC power converter," in *Proc. IPEC-ECCE Asia*, Jeju, South Korea, May 30–Jun. 3, 2011. [CD-ROM].

[25] C. P. Steinmetz, "On the law of hysteresis," *Proc. IEEE*, vol. 72, no. 2, pp. 196–221, Feb. 1984.

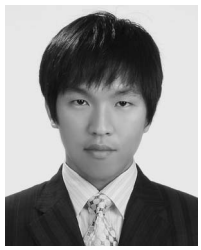

Myoungho Kim (S'09) was born in Seoul, Korea, in 1984. He received the B.S. degree in electrical engineering from Hanyang University, Seoul, in 2006, and the M.S. degree in electrical engineering from Seoul National University, Seoul, in 2008, where he is currently working toward the Ph.D. degree.

His research interests include high-performance ac drive systems, and high-power converter design and control.

Anno Yoo (S'07–M'10) was born in Seoul, Korea, in 1977. He received the B.S., M.S., and Ph.D. degrees in electrical engineering from Seoul National University, Seoul, in 2004, 2006, and 2010, respectively.

Since 2010, he has been a Senior Research Engineer with LSIS Co., Ltd., Anyang-si, Korea. His current interests include high-performance ac drive systems, high-power converter design, and electric/hybrid vehicle drives.

Seung-Ki Sul (S'78–M'80–SM'98–F'00) was born in Korea in 1958. He received the B.S., M.S., and Ph.D. degrees in electrical engineering from Seoul National University, Seoul, Korea, in 1980, 1983, and 1986, respectively.

From 1986 to 1988, he was an Associate Researcher in the Department of Electrical and Computer Engineering, University of Wisconsin, Madison. From 1988 to 1990, he was a Principal Research Engineer with Gold-Star Industrial Systems Company. Since 1991, he has been a Professor of the School of Electrical Engineering and Computer Science, Seoul National University, where he was the Vice Dean from 2005 to 2007, and was the President of the Korea Electrical Engineering and Science Research Institute from 2008 to 2011. His current research interests are power-electronic control of electric machines, electric/hybrid vehicle drives, and power-converter circuits.